GENE THERAPY

Systemic AAV9.LAMP2B injection reverses metabolic and physiologic multiorgan dysfunction in a murine model of Danon disease

Ana Maria Manso[1], Sherin I. Hashem[2]*, Bradley C. Nelson[1]*, Emily Gault[1], Angel Soto-Hermida[1], Elizza Villarruel[1], Michela Brambatti[1], Julius Bogomolovas[1], Paul J. Bushway[1], Chao Chen[1], Pavan Battiprolu[3], Annahita Keravala[3], Jonathan D. Schwartz[3], Gaurav Shah[3], Yusu Gu[1], Nancy D. Dalton[1], Kirk Hammond[1], Kirk Peterson[1], Paul Saftig[4], Eric D. Adler[1]†

Danon disease (DD) is a rare X-linked autophagic vacuolar myopathy associated with multiorgan dysfunction, including the heart, skeletal muscle, and liver. There are no specific treatments, and most male patients die from advanced heart failure during the second or third decade of life. DD is caused by mutations in the lysosomal-associated membrane protein 2 (*LAMP2*) gene, a key mediator of autophagy. LAMP2 has three isoforms: LAMP2A, LAMP2B, and LAMP2C. LAMP2B is the predominant isoform expressed in cardiomyocytes. This study evaluates the efficacy of human *LAMP2B* gene transfer using a recombinant adeno-associated virus 9 carrying human LAMP2B (AAV9.LAMP2B) in a *Lamp2* knockout (KO) mouse, a DD model. AAV9.LAMP2B was intravenously injected into 2- and 6-month-old *Lamp2* KO male mice to assess efficacy in adolescent and adult phenotypes. *Lamp2* KO mice receiving AAV9.LAMP2B demonstrated dose-dependent restoration of human LAMP2B protein in the heart, liver, and skeletal muscle tissue. Impaired autophagic flux, evidenced by increased LC3-II, was abrogated by *LAMP2B* gene transfer in all tissues in both cohorts. Cardiac function was also improved, and transaminases were reduced in AAV9.LAMP2B-treated KO mice, indicating favorable effects on the heart and liver. Survival was also higher in the older cohort receiving high vector doses. No anti-LAMP2 antibodies were detected in mice that received AAV9.LAMP2B. In summary, *LAMP2B* gene transfer improves metabolic and physiologic function in a DD murine model, suggesting that a similar therapeutic approach may be effective for treating patients with this highly morbid disease.

INTRODUCTION

Danon disease (DD) is a rare, X-linked autophagic vacuolar myopathy caused by loss-of-function mutations in the gene encoding lysosomal-associated membrane protein type 2 (LAMP2), a lysosomal transmembrane protein critical for autophagy (*1*). DD is the only human cardiomyopathy known to be caused by mutations in a lysosomal transmembrane protein (*1*, *2*). Penetrance of disease-causing mutations in DD is nearly 100% in males, and the cardiac phenotype is severe (*3*). Most male patients develop severe cardiac hypertrophy and arrhythmias in early adolescence. In addition to cardiomyopathy, patients also suffer from liver dysfunction, skeletal myopathies, retinal disease, and cognitive impairment. Transaminases are frequently elevated in male patients, although limited clinical liver dysfunction in patients has been reported to date. No specific therapies for the treatment of DD exist, and most patients either die from heart failure or require cardiac transplant by age 30 (*3*). The true prevalence of DD is unknown. Recent registry-based studies of patients with hypertrophic cardiomyopathy (HCM) suggest that *LAMP2* mutations underlie 1 to 4% of HCM (*4*–*8*).

The *LAMP2* gene codes for three alternatively spliced RNA isoforms (*LAMP2A*, *LAMP2B*, and *LAMP2C*) that are distinguishable by a variable transmembrane domain and 13 amino acid cytoplasmic tail. Each isoform has been implicated in a different type of autophagy. LAMP2A plays an essential role in chaperone-mediated autophagy (CMA), and LAMP2C is thought to be involved in RNA and DNA degradation (*9*, *10*). LAMP2B has been associated with macroautophagy (*10*) and is also the predominant LAMP2 isoform expressed in cardiomyocytes (*11*). Because cardiac disease is severe in patients with DD and several patients have been identified with mutations in the exon specifically encoding LAMP2B, this isoform has been postulated to be critical in the pathogenesis of the disease (*11*, *12*). In previous studies, repletion of LAMP2B was sufficient to improve autophagy as well as cardiac metabolic and physiologic function in induced pluripotent stem cell–derived cardiomyocytes (iPSC-CMs) from patients with DD (*13*, *14*).

Recombinant adeno-associated viruses (AAVs) have become a powerful tool for gene-based treatment of a variety of diseases, with broad tissue tropism and absence of known pathogenesis in humans (*15*). AAV serotype 9 (AAV9) has been shown to be highly efficient at delivering genes to major tissues including the liver, heart, skeletal muscle, and central nervous system (*16*–*20*), all affected organs, and tissues in DD.

Here, we evaluate the efficacy of gene transfer of AAV9 carrying the wild-type (WT) human *LAMP2B* complementary DNA (cDNA) (AAV9.LAMP2B) in a previously established mouse model of DD, the *Lamp2* knockout (KO) mouse (*21*). We specifically evaluate the effect of AAV9.LAMP2B for treatment of cardiac, skeletal, and hepatic derangements and determine whether treatment could improve the metabolic and physiologic abnormalities noted in this model.

To investigate the potential of gene therapy for the treatment of DD, we created an AAV9 vector overexpressing human *LAMP2B* (AAV9.LAMP2B) in collaboration with the University of Pennsylvania viral vector core. Transgene expression is under the control of the constitutively active CAG promoter, consisting of a cytomegalovirus

[1]Division of Cardiology, Department of Medicine, UC San Diego, San Diego, CA 92037, USA. [2]Department of Pathology, UC San Diego, San Diego, CA 92037, USA. [3]Rocket Pharmaceuticals, New York, NY 10118, USA. [4]Biochemical Institute, Christian Albrechts-University, Kiel 24118, Germany.
*These authors contributed equally to the work.
†Corresponding author. Email: eradler@health.ucsd.edu

(CMV) enhancer and a chicken β-actin promoter, along with a chimeric chicken β-actin and rabbit globin intron (Fig. 1A). This constitutively active promoter was chosen to allow for LAMP2B isoform expression in multiple tissues because DD is a multiorgan disorder (*22*).

To determine whether AAV9.LAMP2B is efficacious for the treatment of DD, we used an established *Lamp2* KO murine model of DD. These mice accumulate autophagic vacuoles in multiple organs including the heart, skeletal muscle, and liver (*21*, *23*), findings also observed in patients with DD (*3*). Patients with DD typically present initially with extreme HCM, which generally progresses to end-stage heart failure (*3*, *24*). Although *Lamp2* KO mice demonstrate systolic and diastolic dysfunction by invasive hemodynamic studies, earlier work has shown this disease model does not develop the severe cardiac hypertrophy or reduced ejection fraction characteristic of the human disease (*14*, *25*, *26*).

To explore the efficacy of AAV9.LAMP2B, two cohorts of mice were used: 6- and 2-month-old *Lamp2* KO male mice. The 6-month-old cohort was used to determine the therapeutic potential of gene therapy in adult patients with established disease, whereas the 2-month-old cohort was intended to evaluate whether the therapy could prevent disease development and/or progression and to assess treatment durability (fig. S1, A and B). The 6-month-old cohort was evaluated at age of 9 months (12 weeks after treatment), and the 2-month-old cohort was examined at ages of 5 and 8 months (12 and 24 weeks after treatment). Untreated littermate WT mice were used as controls. The mice were intravenously injected with phosphate-buffered saline (PBS) or AAV9.LAMP2B at doses of 1×10^{13}, 5×10^{13}, 1×10^{14}, or 2×10^{14} vector genomes (vg)/kg.

Starvation has been shown to be a potent stimulus for the induction of macroautophagy (*27*), and intermittent fasting is known to stimulate myocardial autophagy, leading to worsening cardiac function in *Lamp2* KO mice (*26*). Thus, all animals were subjected to alternate-day starvation (intermittent fasting) for 6 weeks before final assessment and study termination (fig. S1, A and B).

RESULTS

AAV9.LAMP2B vector was detected in the liver, heart, and skeletal muscle

Vector copy number (VCN) per nuclei was calculated to determine the amount of AAV9.LAMP2B vector in the liver, heart, and skeletal muscle in the 6- and 2-month-old cohorts at 12 and 24 weeks after injection. The differential biodistribution of the vg in the three tissues shows that in both cohorts, the highest vg concentration was detected in the liver, followed by the heart, and the skeletal muscle (table S1), findings that are consistent with previous studies evaluating AAV9 transfection properties (*28*). In the 2-month-old cohort 24 weeks after injection, a dose-dependent difference in biodistribution was observed in the three tissues (table S1).

Systemic delivery of AAV9.LAMP2B vector did not induce detectable evidence of toxicity in *Lamp2* KO mice

To evaluate the potential toxicity of AAV9.LAMP2B vector after systemic delivery, antidrug antibodies (ADAs) were tested in the serum from *Lamp2* KO mice. Specifically, we evaluated the presence of ADAs in 8-month-old mice that were injected at 2 months of age. These mice received doses of either 1×10^{14} vg/kg ($n = 5$) or 2×10^{14} vg/kg ($n = 4$) of AAV9.LAMP2B or PBS ($n = 5$). As expected, antibodies against the viral capsid were detected in both AAV-injected groups in all mice tested (antibody titers $\log_{10}$ values ranged from 4.5 to 5.9). Only one of five mice injected with PBS had detectable antibody and at a lower amount than those injected with AAV9 (antibody titer $\log_{10}$ value, 1.7; table S2). These data confirm the development of antibody after injection of AAV9 and the very low amount of preexisting antibody in *Lamp2* KO mice not exposed to AAV9. We also evaluated the development of antibody to the LAMP2 transgene. Unlike capsid antibodies, only 2 of 10 mice (1 in the 1×10^{14} vg/kg group and 1 in the 2×10^{14} vg/kg) developed antibodies against the transgene. These antibodies were much lower than those against the viral capsid (antibody titer $\log_{10}$ values, 1.7 to 2.0). No antibody to LAMP2 was detected in mice injected with PBS (table S2). Furthermore, histopathologic analysis of the heart, spleen, liver, skeletal muscle, kidney, brain, lung, and testis revealed no adverse microscopic findings (fig. S2), which suggests the lack of deleterious immune response against the AAV9 or the transgene. Therefore, although an immune response was detected against the AAV9 capsid, it was not associated with a detectable toxic response.

Administration of AAV9.LAMP2B results in the high expression of human LAMP2B in the myocardium as well as a decrease in vacuolation and improvement in cardiac function in *Lamp2* KO mice

To establish the efficiency of the *LAMP2B* transgene expression in cardiac muscle in the 6-month-old cohort, we measured the RNA transcript and relative amount of protein of LAMP2 at 12 weeks after AAV9.LAMP2B administration. Because there are no antibodies available that reliably recognize epitopes on both human and mouse LAMP2, we were not able to calculate the amount of protein generated by the AAV9.LAMP2B vector in the injected *Lamp2* KO mice compared with the mouse endogenous LAMP2 protein in WT mice. To overcome this problem, we designed a set of primers that recognize both human and mouse LAMP2 transcripts to calculate and compare LAMP2 transcript in WT (endogenous LAMP2) and AAV9.LAMP2B-injected *Lamp2* KO mice (transcript produced by the transgene). Administration of AAV9.LAMP2B resulted in dose-dependent expression of LAMP2 transcript in cardiac tissue from injected *Lamp2* KO mice, with more than a 20-fold increase in LAMP2 expression in the 5×10^{13}, 1×10^{14}, and 2×10^{14} vg/kg doses compared with WT endogenous amounts (Fig. 1B). Similarly, AAV9.LAMP2B-injected mice showed dose-dependent expression of human LAMP2B protein in the heart tissue (Fig. 1, C and D). Representative images of human LAMP2 expression assessed by immunofluorescence on cardiac tissue (Fig. 1F) demonstrate broadly expression of human LAMP2B in the cytosol of cardiomyocytes at the higher concentrations of AAV9.LAMP2B.

We then sought to determine the impact of AAV9.LAMP2B on cardiac autophagy using molecular and ultrastructural analyses. Microtubule-associated protein 1 light chain 3, usually referred to as LC3, is an essential protein in autophagy, and the accumulation of its lipid modified form, referred to as LC3-II, is associated with impaired autophagy (*29*). Previous studies have demonstrated that LAMP2 deficiency leads to dysregulation of autophagic flux due to defects in autophagosome-lysosome fusion (*10*, *11*), resulting in an increase in the amount of autophagosome-bound LC3-II in the myocardium of *Lamp2* KO mice (*26*). Consistent with results from those studies, LC3-II band intensity was increased fourfold in cardiac tissue from untreated, PBS-injected *Lamp2* KO mice compared

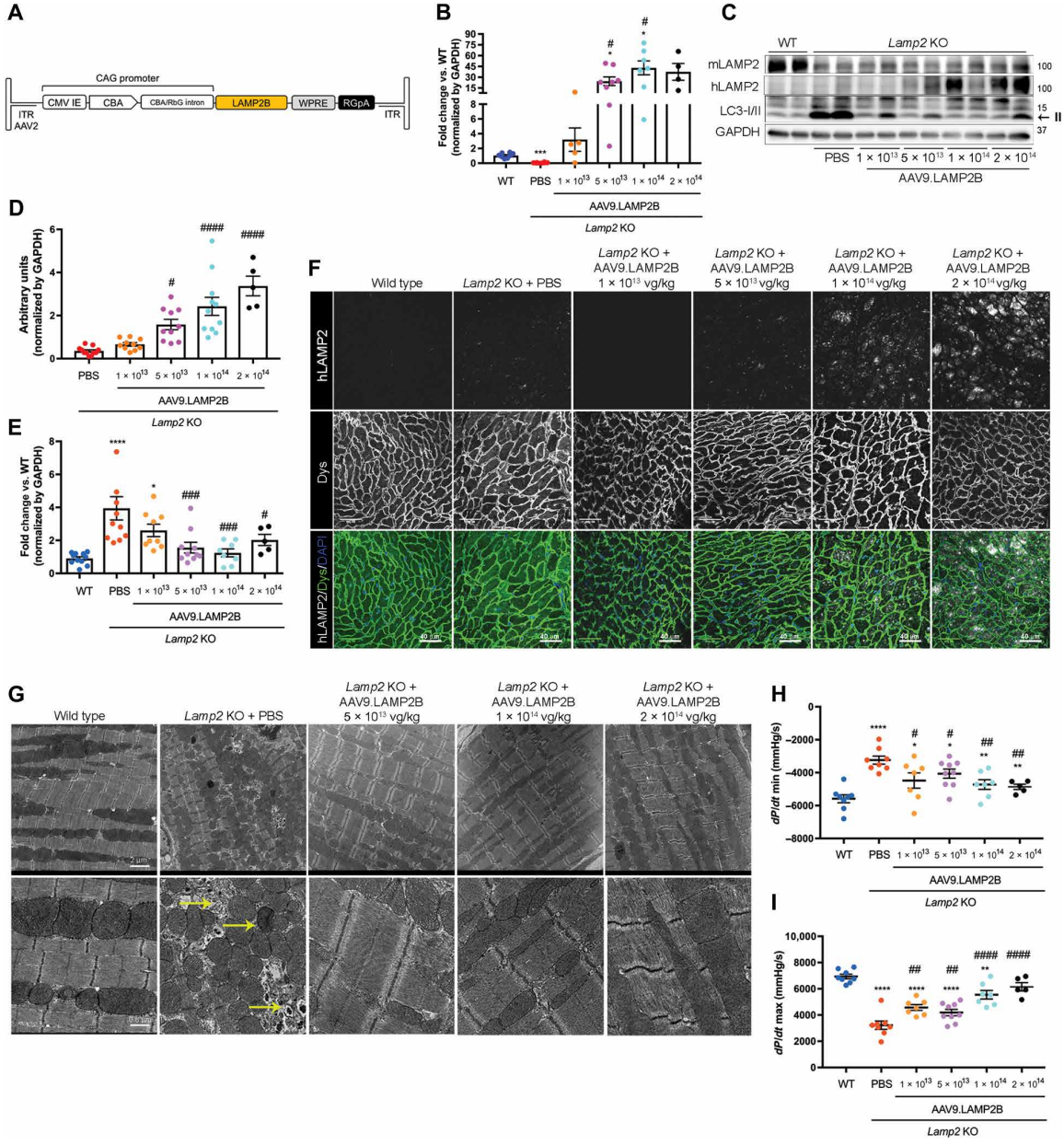

Fig. 1. Administration of AAV9.LAMP2B in adult (6-month-old) mice shows dose-dependent expression of human LAMP2B in heart tissue from *Lamp2* KO mice together with an improvement in autophagic flux and cardiac function. (**A**) The pAAV-*LAMP2B* transfer plasmid (pAAV_CB7.CI.LAMP- 2B.WPRE.rBG) contains this expression cassette flanked by viral ITR regions derived from AAV2. (**B**) Quantitative reverse transcription polymerase chain reaction (qRT-PCR) was used to quantify LAMP2 mRNA transcripts in cardiac tissue from WT ($n = 8$) and *Lamp2* KO mice injected with PBS ($n = 8$) or increasing doses of AAV9.LAMP2B [1×10^{13} vg/kg ($n = 5$), 5×10^{13} vg/kg ($n = 8$), 1×10^{14} vg/kg ($n = 7$), and 2×10^{14} vg/kg ($n = 4$)]. Glyceraldehyde-3-phosphate dehydrogenase (GAPDH) was used as a reference gene for internal normalization. Data are means ± SEM. ***$P < 0.001$, *$P < 0.05$ versus WT; #$P < 0.05$ versus PBS. Statistical analysis was performed using Welch's ANOVA. (**C**) Protein lysates from the cardiac tissue of *Lamp2* KO mice treated with PBS or increasing doses of AAV9.LAMP2B (1×10^{13}, 5×10^{13}, 1×10^{14}, and 2×10^{14} vg/kg) and control WT mice were evaluated by Western blot for mouse and human LAMP2 (mLAMP2 and hLAMP2, respectively) and LC3-II. GAPDH was used as a loading control. (**D**) Quantification of human LAMP2 (arbitrary units normalized to GAPDH). *Lamp2* KO injected with AAV9.LAMP2B [1×10^{13} vg/kg ($n = 10$), 5×10^{13} vg/kg ($n = 10$), 1×10^{14} vg/kg ($n = 11$), and 2×10^{14} vg/kg ($n = 5$)]. Data are means ± SEM. ####$P < 0.0001$ and #$P < 0.05$ versus PBS. Statistical analysis was performed using one-way ANOVA. (**E**) Quantification of LC3-II (fold change over WT) normalized to GAPDH. WT ($n = 11$) and *Lamp2* KO injected with PBS ($n = 11$) or increasing doses of AAV9.LAMP2B [1×10^{13} vg/kg ($n = 9$), 5×10^{13} vg/kg ($n = 10$), 1×10^{14} vg/kg ($n = 8$), and 2×10^{14} vg/kg ($n = 5$)]. Data are means ± SEM. ****$P < 0.0001$, *$P < 0.05$ versus WT; ###$P < 0.001$, #$P < 0.05$ versus PBS. Statistical analysis was performed using one-way ANOVA. (**F**) Representative human LAMP2 immunofluorescence staining of heart sections from WT and *Lamp2* KO mice treated with PBS or AAV9.LAMP2B (1×10^{13}, 5×10^{13}, 1×10^{14}, and 2×10^{14} vg/kg). Dystrophin (Dys) was used to mark and localize cardiac myocytes. DAPI, 4′,6-diamidino-2-phenylindole. (**G**) Representative transmission electron microscopy images of cardiac tissue from WT and *Lamp2* KO mice treated with AAV9.LAMP2B. Autophagy structures are indicated with yellow arrows. (**H**) *dP/dt* max (rate of rise of left ventricular pressure; contractility) and (**I**) *dP/dt* min (rate of fall of left ventricular pressure; relaxation). WT ($n = 8$). *Lamp2* KO injected with PBS ($n = 8$) or increasing doses of AAV9.LAMP2B [1×10^{13} vg/kg ($n = 7$), 5×10^{13} vg/kg ($n = 9$), 1×10^{14} vg/kg ($n = 7$), and 2×10^{14} vg/kg ($n = 5$)]. Values are means ± SEM. ****$P < 0.001$, **$P < 0.01$, *$P < 0.05$ versus WT; #$P < 0.05$, ##$P < 0.01$, and ####$P < 0.0001$ versus PBS. Statistical analysis was performed using one-way ANOVA.

with WT controls. Administration of AAV9.LAMP2B was associated with a dose-dependent reduction in LC3-II compared with PBS-injected mice as measured by Western blot. Band intensity between the treated mice was similar to WT mice at the 5×10^{13} and 1×10^{14} vg/kg doses, suggesting rescue of autophagy in *Lamp2* KO mice receiving AAV9.LAMP2B (Fig. 1, C and E). To evaluate the myocardial ultrastructure of *Lamp2* KO mice, we performed electron microscopy on cardiac tissue. Representative transmission electron microscopy images 12 weeks after injection are shown in Fig. 1G. Autophagic structures were noted throughout the cytosol of untreated LAMP2B KO (arrows in Fig. 1G); these findings were not noted in AAV9.LAMP2B-injected *Lamp2* KO mice or WT controls.

One of the limitations of the DD mouse model is the lack of detectable cardiac hypertrophy or reduction in ejection fraction (*14*). Similarly, we noted no difference in cardiac structure, fibrosis, or ejection fraction in any of the cohorts (see tables S3 and S4 and fig. S3). Despite this limitation, our previous work indicated a reduction in cardiac contractile function by invasive hemodynamic studies (*14*). Hence, we performed invasive hemodynamic studies on mice 12 weeks after injection of AAV9.LAMP2B. Cardiac contraction and relaxation as evaluated by *dP*/*dt* max, *dP*/*dt* min (positive and negative first derivatives for maximal rates of left ventricular pressure development, respectively), and Tau (left ventricular relaxation time constant) were improved in a dose-dependent manner up to 2×10^{14} vg/kg in the AAV9.LAMP2B-treated *Lamp2* KO mice compared with PBS-injected controls at all doses tested (Fig. 1, H and I, and table S5A) but are still different than WT mice. These data demonstrate that AAV9.LAMP2B ameliorates some of the physiologic and metabolic cardiac dysfunction in older mice with an established DD phenotype.

To assess treatment durability and evaluate the efficacy of the AAV9.LAMP2B vector in adolescents, we injected 2-month-old *Lamp2* KO male mice and evaluated them at 12 and 24 weeks after treatment for vector genomes and LAMP2 transcript in cardiac tissue. No changes in VCN and LAMP2 mRNA transcripts were seen between 12 and 24 weeks after injection (fig. S4, A and B), indicating the persistence of the vector genomes and sustained transgene expression in the heart.

Similar to the older cohort, administration of AAV9.LAMP2B resulted in dose-dependent expression of LAMP2 transcript and protein in the cardiac tissue of treated *Lamp2* KO mice 24 weeks after infection (Fig. 2, A to C). Representative images shown in Fig. 2E demonstrated a pattern similar to the older cohort, with expression throughout the cytosol of myocytes of treated *Lamp2* KO mice at the higher AAV9.LAMP2B concentrations. In parallel with increased LAMP2 expression, decreases in LC3-II was seen in AAV9.LAMP2B-injected *Lamp2* KO mice relative to PBS controls (Fig. 2, B and D), suggesting restoration of autophagic flux. Representative transmission electron microscopy images 24 weeks after injection are shown in Fig. 2F and fig. S5. As in the other cohort, autophagic structures were noted throughout the cytosol of untreated *Lamp2* KO (Fig. 2F). Again, we did not note these findings in AAV9.LAMP2B mice or WT controls.

As observed in the 6-month-old cohort, AAV9.LAMP2B administration improved cardiac contraction and relaxation in the 2-month-old cohort, as evaluated by *dP*/*dt* max and *dP*/*dt* min, in a dose-dependent manner (Fig. 2, G to H, and table S5B), although remained different than WT mice (lower *dP*/*dt* max and higher *dP*/*dt* min, respectively).

Together, these data indicate that AAV9.LAMP2B gene transfer improves cardiac metabolic and physiologic function in the DD mouse model. The data also demonstrate persistent treatment effects up to 6 months after injection, indicating the durability of the therapy.

AAV9.LAMP2B therapy results in the high expressions of human LAMP2B in the liver together with an improvement in autophagic flux, liver structure, and hepatic damage in *Lamp2* KO

Liver involvement has previously been reported in animal models of DD (*21*, *30*) and in patients with DD, with many males having elevated serum measurement of liver transaminases [aspartate aminotransferase (AST) and alanine aminotransferase (ALT)] (*3*, *23*). More specifically, *Lamp2* KO mice have been shown to display massive autophagic vacuolar accumulation in the liver (*10*, *21*), although liver function has not been fully evaluated in these mice. In a recent study, *Lamp2* KO rats also displayed a similar accumulation of autophagic vacuoles and increased serum measurements of alkaline phosphatase (ALP), ALT, and AST, potentially indicating liver damage (*31*).

As we observed in our biodistribution data (table S1), AAV9 is known to robustly transduce the liver. We evaluated the effect of AAV9.LAMP2B on hepatic structure and function in *Lamp2* KO mice to see whether these hepatic abnormalities could be corrected and to assess potential hepatotoxic effects of viral vector transduction and/or transgene expression.

First, we evaluated the efficacy of AAV9.LAMP2B to transduce hepatocytes in the 6-month-old cohort. Increases in LAMP2 transcript and human LAMP2B protein were observed in mice treated with AAV9.LAMP2B for 12 weeks (Fig. 3, A to C). Representative images (Fig. 3E) show human LAMP2 expressed throughout the cytosol of hepatocytes of AAV9.LAMP2B-treated *Lamp2* KO mice.

We then determined the effect of AAV9.LAMP2B on liver autophagy. As in the heart, LC3-II protein band intensity was increased fourfold in the liver tissue from PBS-injected *Lamp2* KO mice compared with WT controls (Fig. 3, B and D). Administration of AAV9.LAMP2B was associated with a reduction in LC3-II compared with PBS-injected mice at all doses and were similar to WT at the 5×10^{13} vg/kg dose, confirming the correction of autophagy in the livers of treated *Lamp2* KO mice (Fig. 3, B and D). Representative electron microscopy shown in Fig. 3F shows numerous autophagic vacuoles in the liver tissue from PBS-injected *Lamp2* KO mice, but not in AAV9.LAMP2B mice or WT controls.

AAV9.LAMP2B injection reduced serum ALP and ALT compared with PBS-injected *Lamp2* KO mice (Fig 3, G and H). ALP and ALT were reduced by 51 and 64% in 1×10^{13} vg/kg, 54 and 59% in 5×10^{13} vg/kg, 50 and 76% in 1×10^{14} vg/kg, and 44 and 57% in 2×10^{14} vg/kg treated KO mice, suggesting a reduction in liver damage with treatment. The reduction in liver enzymes further supports the potential therapeutic effect of AAV9.LAMP2B on the liver pathology observed in *Lamp2* KO mice. Histologic studies demonstrate increased hepatic fibrosis in the 9-month-old *Lamp2* KO mice in comparison to WT mice, as assessed by Sirius Red. There was no substantial difference in hepatic fibrosis in the *Lamp2* KO mice in comparison to any of the AAV9.4 LAMP2 cohorts (Fig 3, I and J), suggesting a lack of toxicity to AAV9.LAMP2B administration even at higher doses (1×10^{14} vg/kg).

Although clinical studies have demonstrated that AAV-mediated transduction may result in sustained expression of the therapeutic

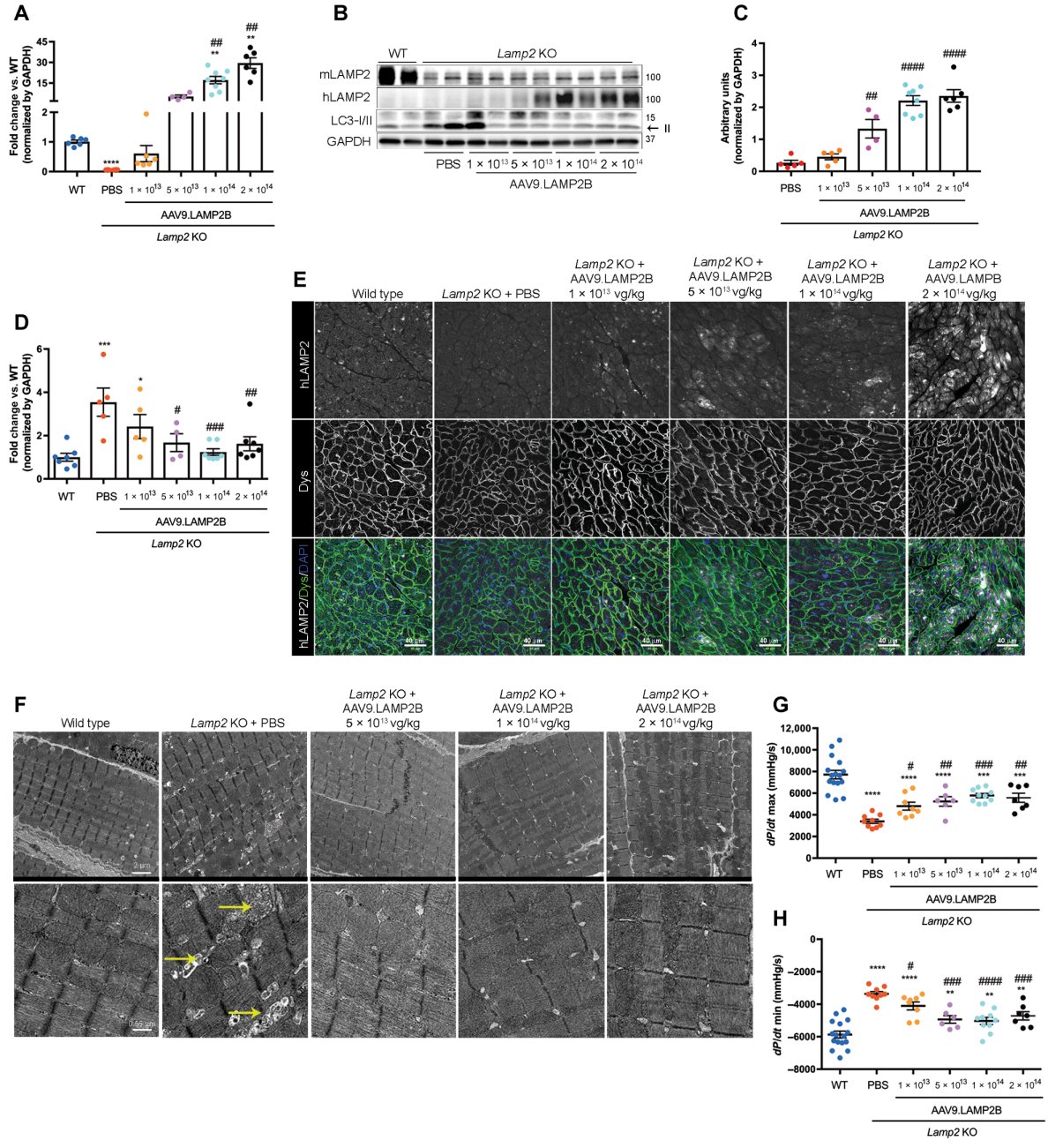

Fig. 2. Administration of AAV9.LAMP2B in adolescent (2-month-old) mice shows dose-dependent expression of human LAMP2B in the heart tissue from *Lamp2* KO mice together with an improvement in autophagic flux and cardiac function. (**A**) qRT-PCR was used to quantify LAMP2 mRNA transcripts in cardiac tissue from WT ($n = 6$) and *Lamp2* KO mice injected with PBS ($n = 6$) or increasing doses of AAV9.LAMP2B [1×10^{13} vg/kg ($n = 6$), 5×10^{13} vg/kg ($n = 4$), 1×10^{14} vg/kg ($n = 8$), and 2×10^{14} vg/kg ($n = 6$)]. GAPDH was used for normalization. Data are means ± SEM. $^{**}P < 0.01$, $^{****}P < 0.0001$ versus WT; $^{\#\#}P < 0.01$ versus PBS. Statistical analysis was performed using Welch's ANOVA. (**B**) Protein lysates from the cardiac tissue of *Lamp2* KO mice treated with PBS or increasing doses of AAV9.LAMP2B (1×10^{13}, 5×10^{13}, 1×10^{14}, and 2×10^{14} vg/kg) and control WT mice were evaluated by Western blot for mouse and human LAMP2 and LC3-II. GAPDH was used as a loading control. (**C**) Quantification of human LAMP2 (arbitrary units normalized to GAPDH). *Lamp2* KO injected with AAV9.LAMP2B [1×10^{13} vg/kg ($n = 5$), 5×10^{13} vg/kg ($n = 4$), 1×10^{14} vg/kg ($n = 8$), and 2×10^{14} vg/kg ($n = 6$)]. Data are means ± SEM. $^{\#\#}P < 0.01$ and $^{\#\#\#\#}P < 0.0001$ versus PBS. Statistical analysis was performed using one-way ANOVA. (**D**) Quantification of LC3-II (fold change over WT) normalized to GAPDH. WT ($n = 7$) and *Lamp2* KO injected with PBS ($n = 5$) or increasing doses of AAV9.LAMP2B [1×10^{13} vg/kg ($n = 5$), 5×10^{13} vg/kg ($n = 4$), 1×10^{14} vg/kg ($n = 7$), and 2×10^{14} vg/kg ($n = 7$)]. Data are means ± SEM. $^{*}P < 0.05$, $^{***}P < 0.001$ versus WT; $^{\#}P < 0.05$, $^{\#\#}P < 0.01$, and $^{\#\#\#}P < 0.001$ versus PBS. Statistical analysis was performed using one-way ANOVA. (**E**) Representative human LAMP2 immunofluorescence staining of heart sections from WT and *Lamp2* KO mice treated with PBS or AAV9.LAMP2B (1×10^{13}, 5×10^{13}, 1×10^{14}, and 2×10^{14} vg/kg). Dystrophin was used to mark and localize cardiac myocytes. (**F**) Representative transmission electron microscopy images of cardiac tissue from WT and *Lamp2* KO mice treated with AAV9.LAMP2B. Autophagy structures are indicated with yellow arrows. (**G**) *dP/dt* max (rate of rise of left ventricular pressure; contractility) and (**H**) *dP/dt* min (rate of fall of left ventricular pressure; relaxation). WT ($n = 16$); *Lamp2* KO injected with PBS ($n = 9$) or increasing doses of AAV9.LAMP2B [1×10^{13} vg/kg ($n = 8$), 5×10^{13} vg/kg ($n = 6$), 1×10^{14} vg/kg ($n = 10$), and 2×10^{14} vg/kg ($n = 7$)]. Values are means ± SEM. $^{**}P < 0.01$, $^{***}P < 0.001$, $^{****}P < 0.0001$ versus WT; $^{\#}P < 0.05$, $^{\#\#}P < 0.01$, $^{\#\#\#}P < 0.001$, and $^{\#\#\#\#}P < 0.0001$ versus PBS. Statistical analysis was performed using one-way ANOVA.

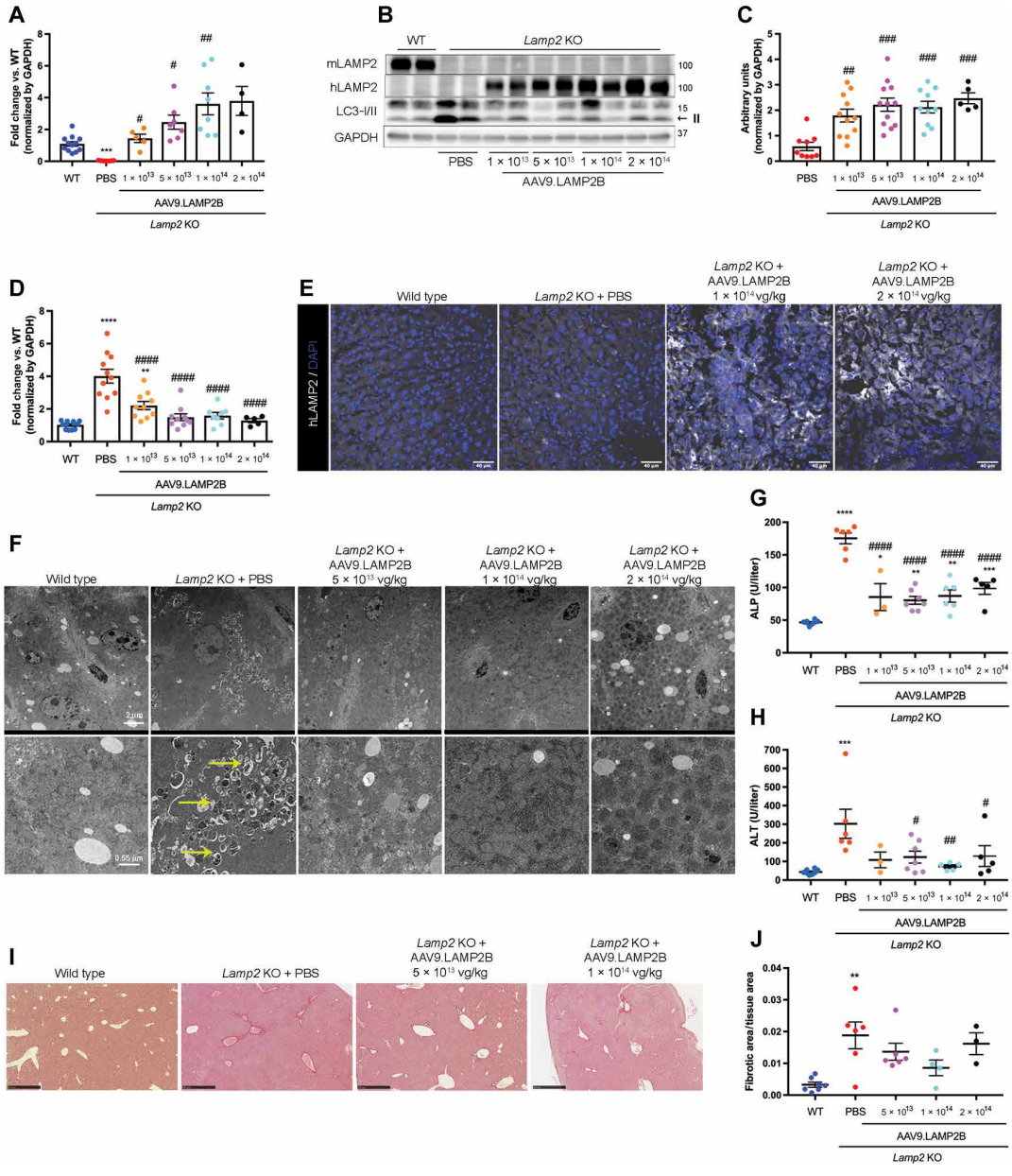

Fig. 3. Administration of AAV9.LAMP2B in adult (6-month-old) mice shows dose-dependent transcription of RNA and expression of human LAMP2B protein in the liver from *Lamp2* KO mice and an improvement in autophagic flux and in the serum ALP and ALT. (**A**) qRT-PCR was used to quantify LAMP2 mRNA transcripts in liver tissue from WT ($n = 12$) and *Lamp2* KO mice injected with PBS ($n = 7$) or increasing doses of AAV9.LAMP2B [1×10^{13} vg/kg ($n = 5$), 5×10^{13} vg/kg ($n = 7$), 1×10^{14} vg/kg ($n = 8$), and 2×10^{14} vg/kg ($n = 4$)]. GAPDH was used for normalization. Data are means ± SEM. ***$P < 0.001$ versus WT; ##$P < 0.01$ and #$P < 0.05$ versus PBS. Statistical analysis was performed using Welch's ANOVA. (**B**) Protein lysates from liver tissue of *Lamp2* KO mice treated with PBS or increasing doses of AAV9.LAMP2B (1×10^{13}, 5×10^{13}, 1×10^{14}, and 2×10^{14} vg/kg) and control WT mice were evaluated by Western blot for mouse and human LAMP2 and LC3-II. GAPDH was used as a loading control. (**C**) Quantification of human LAMP2 (arbitrary units normalized to GAPDH). *Lamp2* KO injected with AAV9.LAMP2B [1×10^{13} vg/kg ($n = 11$), 5×10^{13} vg/kg ($n = 12$), 1×10^{14} vg/kg ($n = 10$), and 2×10^{14} vg/kg ($n = 5$)]. Data are means ± SEM. ###$P < 0.001$ and ##$P < 0.01$ versus PBS. Statistical analysis was performed using one-way ANOVA. (**D**) Quantification of LC3-II (fold change over WT) normalized to GAPDH. WT ($n = 12$) and *Lamp2* KO injected with PBS ($n = 11$) or increasing doses of AAV9.LAMP2B [1×10^{13} vg/kg ($n = 10$), 5×10^{13} vg/kg ($n = 10$), 1×10^{14} vg/kg ($n = 8$), and 2×10^{14} vg/kg ($n = 5$)]. Data are means ± SEM. **$P < 0.01$, ****$P < 0.001$ versus WT; ####$P < 0.001$ versus PBS. Statistical analysis was performed using one-way ANOVA. (**E**) Representative human LAMP2 immunofluorescence staining of liver sections from WT and *Lamp2* KO mice treated with PBS or AAV9.LAMP2B (1×10^{14} and 2×10^{14} vg/kg). (**F**) Representative transmission electron microscopy images of liver tissue from WT and *Lamp2* KO mice treated with AAV9.LAMP2B. Massive accumulation of autophagy structures (indicated with yellow arrows) was decreased in liver from *Lamp2* KO mice after AAV9.LAMP2B administration. (**G**) Alkaline phosphatase (ALP) and (**H**) alanine aminotransferase (ALT) enzymes in serum were blunted in *Lamp2* KO mice after AAV9.LAMP2B administration. WT ($n = 8$) and *Lamp2* KO injected with PBS ($n = 6$) or increasing doses of AAV9.LAMP2B [1×10^{13} vg/kg ($n = 3$), 5×10^{13} vg/kg ($n = 7$), 1×10^{14} vg/kg ($n = 6$), and 2×10^{14} vg/kg ($n = 5$)]. Data are means ± SEM. *$P < 0.05$, **$P < 0.01$, ***$P < 0.001$, ****$P < 0.0001$ versus WT; #$P < 0.05$, ##$P < 0.01$, and ####$P < 0.0001$ versus PBS. Statistical analysis was performed using one-way ANOVA. (**I**) Representative Sirius Red staining of liver tissue from WT and *Lamp2* KO mice treated with PBS or AAV9.LAMP2B (5×10^{13} and 1×10^{14} vg/kg). (**J**) Quantification of Sirius Red–positive areas from WT ($n = 7$) and *Lamp2* KO mice injected with PBS ($n = 6$) or increasing doses of AAV9.LAMP2B [5×10^{13} vg/kg ($n = 6$), 1×10^{14} vg/kg ($n = 4$), and 2×10^{14} vg/kg ($n = 3$)]. The results are presented as area stain for collagen versus tissue area. Data are means ± SEM. **$P < 0.01$ versus WT. Statistical analysis was performed using one-way ANOVA.

protein, durability of expression remains an important question, especially in hepatic tissue (*19*, *32*). To assess treatment durability of the AAV9.LAMP2B vector in younger animals, we injected 2-month-old *Lamp2* KO male mice and evaluated them at 12 and 24 weeks after treatment for VCN and LAMP2 transcript in hepatic tissue. VCN was reduced in the liver 24 weeks after injection compared with 12 weeks, although the VCN values remained substantial and the LAMP2 transcript amounts did not change (fig. S6, A and B). To assess the durability of the efficacious response, we also evaluated the effect of treatment on liver autophagy and function in *Lamp2* KO mice injected at 2 months of age and euthanized 24 weeks after treatment. Similar to the 6-month-old cohort, administration of

AAV9.LAMP2B resulted in increased expression of LAMP2 transcript and protein in the liver tissue from injected *Lamp2* KO mice (fig. S7, A to C). Immunofluorescence analysis (fig. S7E) also showed a pattern similar to the previous cohort with broad expression throughout the liver of treated *Lamp2* KO mice. Decreased LC3-II protein and reduction in autophagic vacuolar accumulation were also seen in the liver tissue from AAV9.LAMP2B-injected *Lamp2* KO mice compared with PBS-injected controls, corroborating the correction in autophagy (fig. S7, D and F). In addition, AAV9.LAMP2B treatment reduced serum ALP and ALT (fig. S7, G and H). Relative to PBS-injected mice, ALP was reduced by 56, 47, 51, and 54% at 1×10^{13}, 5×10^{13}, 1×10^{14}, and 2×10^{14} vg/kg doses, respectively. ALT was reduced by 65, 60, 75, and 76% at 1×10^{13}, 5×10^{13}, 1×10^{14}, and 2×10^{14} vg/kg doses, respectively, compared with PBS-injected mice. This reduction in transaminases suggests an improvement in liver impairment with AAV9.LAMP2B treatment.

To evaluate whether the absence of LAMP2 affected viral transduction in the liver, we compared the VCN of AAV9.LAMP2B in a cohort of WT and *Lamp2* KO mice injected with 2×10^{14} vg/kg. The VCN and human LAMP2 mRNA and protein were lower in the livers of *Lamp2* KO AAV9.LAMP2B-injected mice compared with WT-injected mice. This is in contrast to findings in the heart and skeletal muscle of these mice where we found no differences in vector transduction and transgene expression in *Lamp2* KO mice compared with WT animals (fig. S8). Collectively, these data indicate that AAV9.LAMP2B gene transfer may ameliorate hepatic damage through 6 months after injection in a mouse model of DD.

AAV9.LAMP2B administration results in moderate expression of human LAMP2B with an improvement in autophagic flux in the muscle of *Lamp2* KO mice

Autophagy is critical for muscle homeostasis, and defects in lysosomal function result in several inherited muscle diseases (*33*), including DD. Skeletal myopathy is usually evident in most male patients with DD who present with muscle weakness and elevated serum measurements of creatine kinase (CK) (*34*). Skeletal muscle biopsies show accumulation of autophagosomes and lysosomal structures known as autophagic vacuoles with sarcolemmal features (AVSFs) accompanied by increased in LC3-II, demonstrating autophagic dysregulation (*34*, *35*). Similar to the human disease, *Lamp2* KO mice display accumulation of autophagosomes, AVSFs, and increased LC3-II protein in skeletal muscle (*34*), but they do not present with elevated serum CK (*21*) or muscle weakness as evaluated by grip strength (*36*).

We evaluated the efficacy of AAV9.LAMP2B to transduce skeletal muscle in the 6-month-old cohort. An increase in LAMP2B transcript was seen only in mice treated with 2×10^{14} vg/kg AAV9.LAMP2B versus PBS controls (Fig. 4A) at the 12-week time point, which was consistent with the biodistribution/VCN data, indicating that higher vector doses are necessary to enable efficient expression of LAMP2B in skeletal muscle compared with the liver and heart. Skeletal muscle from AAV9.LAMP2B-injected *Lamp2* KO mice demonstrated evidence of LAMP2 protein expression (Fig. 4, B and C).

In addition, we determined the effect of AAV9.LAMP2B on skeletal muscle autophagy. LC3-II band intensity increased sevenfold in the skeletal muscle tissue from PBS-injected *Lamp2* KO mice compared with WT controls, confirming impaired autophagy (Fig. 4, B and D). Administration of AAV9.LAMP2B was associated with a reduction in LC3-II relative to PBS-injected mice starting at 5×10^{13} vg/kg, indicating restoration of autophagy in the skeletal muscle (Fig. 4, B and D). Representative electron microscopic images are shown in Fig. 4E and reveal an accumulation of autophagic structures in the skeletal muscle, primarily in the tissue from PBS-injected *Lamp2* KO mice in comparison to the other treatment groups.

To determine the durability of AAV9.LAMP2B treatment in the skeletal muscle, we injected 2-month-old *Lamp2* KO male mice and evaluated them at 12 and 24 weeks after treatment for VCN and LAMP2 transcript. No changes in VCN and LAMP2 mRNA were seen between 12 and 24 weeks after injection (fig. S9, A and B), which support the persistence of the vector genome and the expression of the transgene over time in the skeletal muscle. Similar to the 6-month-old cohort, administration of AAV9.LAMP2B resulted in increased expression of LAMP2B transcript at 1×10^{14} vg/kg in comparison to the PBS-treated group (fig. S10A) 24 weeks after infection. LAMP2 protein in the skeletal muscle from AAV9.LAMP2B-injected *Lamp2* KO mice was increased in comparison to the PBS at only the two highest doses (fig. S10, B and C).

Next, we evaluated the impact of AAV9.LAMP2B on skeletal muscle autophagic flux. Expression of human LAMP2 in the skeletal muscle of AAV9.LAMP2B-injected mice was observed at the 1×10^{14} and 2×10^{14} vg/kg doses of AAV9. Decreased LC3-II band intensity was noted in the skeletal muscle from AAV9.LAMP2B-treated mice compared with PBS-injected controls (fig. S10D). Representative images (immunofluorescence and electron microscopy) are shown in fig. S10 (E and F) and show numerous autophagic vacuoles, primarily in untreated mice.

These data indicate improved autophagic flux in *Lamp2* KO mice receiving the highest doses of AAV9.LAMP2B. Overall, AAV9.LAMP2B transduction was less extensive in the skeletal muscle compared with the heart or liver.

Improved survival of treated *Lamp2* KO mice

Homozygous patients with DD have a shortened life span (*24*). In this study, *Lamp2* KO mice receiving AAV9.LAMP2B at doses of 5×10^{13}, 1×10^{14}, and 2×10^{14} vg/kg in the 6-month-old cohort showed increased survival compared with PBS-injected controls (fig. S11A); however, the cause of death could not be ascertained. On the contrary, the mice from the 2-month-old cohort did not show difference in mortality by the time of sacrifice (fig. S11B). Because the mouse cohorts in this study were euthanized at a predetermined end point, dedicated survival studies will be required to confirm our findings.

DISCUSSION

DD is a devastating multisystemic disorder for which no specific treatment is available. For several reasons, genetic therapy has considerable therapeutic potential in this monogenic disorder: DD is highly penetrant in patients with *LAMP2* mutations, the protein is relatively small and can readily be "packaged" in AAV, and the disease is multisystemic and, thus, single-organ transplantation as a definitive treatment is not sufficient. Preclinical and clinical studies of AAV9 suggest that this vector can be administered safely with minimal risk of toxicity in therapeutic ranges (*15*).

We explored the efficacy of AAV9.LAMP2B in a previously established *Lamp2* KO murine model of the disease. We used caloric restriction to stimulate autophagy in these mice, which may otherwise have relatively low rates of basal autophagy given continuous access

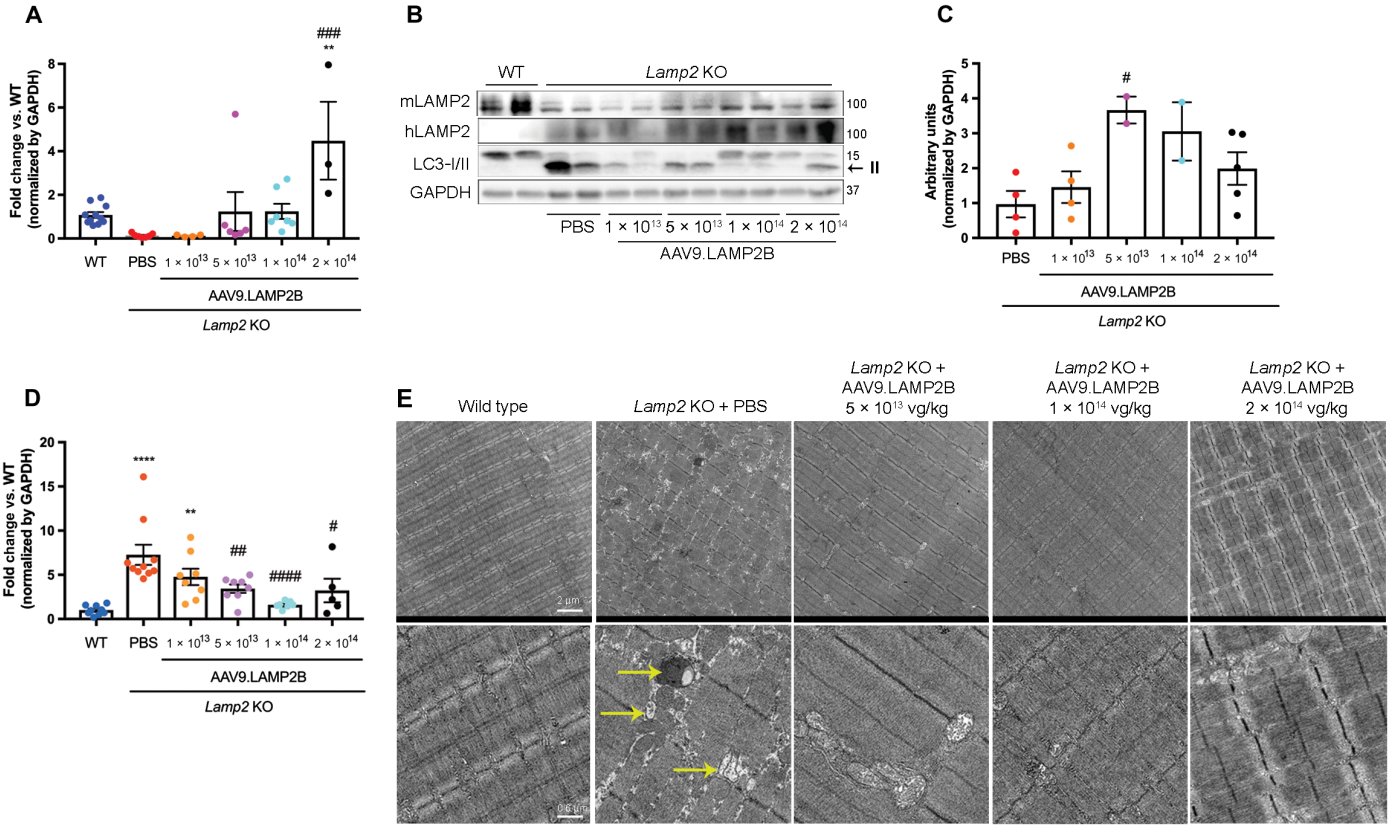

Fig. 4. Administration of AAV9.LAMP2B in adult (6-month-old) mice shows dose-dependent expression of human LAMP2B in skeletal muscle from *Lamp2* KO mice together with an improvement in autophagic flux. (**A**) qRT-PCR was used to quantify LAMP2 mRNA transcripts in skeletal muscle from WT ($n = 11$) and *Lamp2* KO injected with PBS ($n = 7$) or increasing doses of AAV9.LAMP2B [1×10^{13} vg/kg ($n = 4$), 5×10^{13} vg/kg ($n = 6$), 1×10^{14} vg/kg ($n = 7$), and 2×10^{14} vg/kg ($n = 3$)]. GAPDH was used for normalization. Data are means ± SEM. $^{**}P < 0.01$ versus WT; $^{\#\#\#}P < 0.001$ versus PBS. Statistical analysis was performed using one-way ANOVA. (**B**) Protein lysates from the cardiac tissue of *Lamp2* KO mice treated with PBS or increasing doses of AAV9.LAMP2B [1×10^{13}, 5×10^{13}, 1×10^{14}, and 2×10^{14} vg/kg) and control WT mice were evaluated by Western blot for mouse and human LAMP2 and LC3-II. GAPDH was used as a loading control. (**C**) Quantification of human LAMP2 (arbitrary units normalized to GAPDH). *Lamp2* KO injected with AAV9.LAMP2B [1×10^{13} vg/kg ($n = 14$), 5×10^{13} vg/kg ($n = 2$), 1×10^{14} vg/kg ($n = 2$), and 2×10^{14} vg/kg ($n = 5$)]. Data are means ± SEM. $^{\#}P < 0.05$ versus PBS. Statistical analysis was performed using one-way ANOVA. (**D**) Quantification of LC3-II (fold changeover WT) normalized to GAPDH. WT ($n = 9$) and *Lamp2* KO injected with PBS ($n = 10$) or increasing doses of AAV9.LAMP2B [1×10^{13} vg/kg ($n = 8$), 5×10^{13} vg/kg ($n = 8$), 1×10^{14} vg/kg ($n = 7$), and 2×10^{14} vg/kg ($n = 5$)]. Data are means ± SEM. $^{**}P < 0.01$, $^{****}P < 0.0001$ versus WT; $^{\#}P < 0.05$, $^{\#\#}P < 0.01$, and $^{\#\#\#\#}P < 0.0001$ versus PBS. Statistical analysis was performed using one-way ANOVA. (**E**) Representative transmission electron microscopy images of skeletal muscle tissue from WT and *Lamp2* KO mice treated with AAV9.LAMP2B. Autophagy structures are indicated with yellow arrows.

to food and sedentary activity in captivity. Previous studies have demonstrated a worse cardiac phenotype in mice calorically restricted via alternate-day starvation (*26*). To evaluate the therapeutic effects of AAV9.LAMP2B after the onset of disease, we injected mice at 6 months of age and euthanized them at 9 months. We saw improvement in cardiac and hepatic phenotypes and improvement in autophagy in the heart, liver, and skeletal muscle tissue, suggesting that this therapy may benefit patients with established symptoms of DD. We also saw improved survival in 6-month-old mice receiving the three highest doses of AAV9.LAMP2B, although these findings will require confirmation in dedicated survival studies because our mice were euthanized at a predefined time point.

Subsequently, we explored the effect of AAV9.LAMP2B on 2-month-old mice to evaluate the effect on a younger cohort. As in the 6-month-old group, we demonstrated that AAV9.LAMP2B treatment resulted in expression of LAMP2B RNA that were equivalent to or higher than WT in the heart, liver, and skeletal muscle. Immunoblot using LAMP2B antibodies demonstrated that the protein was expressed in a dose-dependent fashion in the heart. Autophagic flux was improved in all three tissues with treatment. Although previous studies have raised concerns for liver toxicity at high vector doses of systemically delivered AAV (*37*, *38*), in our study, we found no evidence of treatment-related hepatic injury. Circulating hepatic enzyme amounts were markedly reduced in the mice treated with AAV9.LAMP2B. The mechanisms by which LAMP2 deficiency causes elevated liver enzymes are not defined. Both humans and a recently developed rat model of DD have elevated measurements of serum hepatic enzymes in the blood. This may be due to a decrease in macroautophagy of hepatic canalicular proteins (*30*). It may also be due to a decrease in hepatic CMA, as previous studies suggest a critical role of LAMP2 in hepatic CMA (*39*).

Of interest, VCN, human LAMP2 mRNA transcript, and relative protein amounts were lower in the liver from AAV9.LAMP2B-injected *Lamp2* KO mice compared with WT-injected mice 4 weeks after treatment. This may be due to hepatic fibrosis in *Lamp2* KO mice or to a higher hepatocyte proliferation (a likely consequence of hepatic involvement), which could decrease the proportion of vector-transduced cells over time (*40*, *41*). An additional possibility is that

the viral load at this concentration (2×10^{14} vg/kg) could result in greater liver injury in *Lamp2* KO liver compared with WT control, although the negligible immunogenic response and overall reduction in serum enzymes render this unlikely. It appears that administration of AAV9.LAMP2B to both 2-month- and 6-month-old *Lamp2* KO mice improves autophagic flux and liver enzymes.

In previous studies by our group and others, the absence of LAMP2, and specifically LAMP2B, resulted in impaired autophagic flux, increased oxidative stress, reduced mitochondrial respiration, and abnormal calcium handling (*11*, *14*). In vitro models suggest that replacement of LAMP2B resolves these abnormalities in cardiomyocytes derived from patients with DD (*13*). This is consistent with the substantial improvement in cardiac hemodynamic function after treatment with AAV9.LAMP2B. Hence, we believe that impaired autophagy due to the absence of LAMP2B results in impaired cardiac contraction and relaxation; however, further study is required to confirm the precise mechanism of the cardiac pathophysiology observed in our study.

Our results in the *Lamp2* KO mouse model of DD confirmed the durability of LAMP2B transgene expression at 6 months after injection. However, unlike the older group, we did not see a substantial difference in mortality in this (2-month-old) cohort at the time of sacrifice (8 months of age); this may be the result of the age difference between cohorts. Dedicated survival studies are ongoing, as are murine and primate toxicity studies.

It has been previously suggested that LAMP2A is primarily responsible for CMA and that LAMP2B is involved predominantly in macroautophagy (*42*). As stated above, we specifically tested the LAMP2B isoform because human genetic studies indicate that isolated LAMP2B mutations are sufficient to cause disease, whereas no patients have been identified with deficiencies isolated in LAMP2A or LAMP2C. Furthermore, recent studies using iPSC-CMs from patients with DD show restoration of autophagic flux with overexpression of LAMP2B, but not LAMP2A or LAMP2C (*11*).

Our data suggest a direct relationship between vector dose and protein expression, as well as improvement in hemodynamic function and reduction in transaminases. Ultimately, little difference was noted between the 1×10^{14} and 2×10^{14} vg/kg doses, suggesting that 1×10^{14} vg/kg may be a threshold dose for efficacy, although it is uncertain whether this will translate to human studies. Because higher AAV doses may have greater potential for toxicity, identification of the lowest efficacious dose is important but ultimately will be determined by results from ongoing clinical studies.

Our study has certain limitations. The *Lamp2* KO murine model of DD does not fully replicate all of the features of the clinical disorder. These mice do not develop reduced ejection fraction, even with intermittent starvation. Hence, further study, possibly with other model systems and or patient tissue, will be required to help elucidate the intrinsic pathophysiology of the disease. We have also not thoroughly evaluated the neurocognitive impact of AAV9.LAMP2B; this may be particularly challenging using *Lamp2* KO mice, as previous studies using this model system did not demonstrate severe manifestations in the brain that are noted in other organ systems (*36*).

The *Lamp2* KO model used also does not develop significant fibrosis in the heart. Hence, the impact of fibrosis on viral transduction will have to be evaluated in humans or other model systems with cardiac fibrosis. It is feasible that gene therapy will be better suited before the onset of significant fibrosis, although this also will need to be evaluated in clinical studies.

We did not test AAV9.LAMP2B in female mice because heterozygous female mice have no readily evident symptoms and homozygous females are extremely difficult to breed. This is a significant limitation of the animal system studied, especially since female heterozygous patients frequently get DD (*24*), clinical evaluation of AAV9.LAMP2B in female populations will likely be required to enable meaningful assessments of efficacy in this patient population.

Although our data are largely consistent with a dose-response relationship, some of our findings are not entirely consistent regarding this relationship. For example, the *dP*/*dT* max and *dP*/*dT* min readings from KO mice dosed with 1×10^{13} vg/kg as noted in the 6-month-old cohort appear greater than KO mice dosed with 5×10^{13} vg/kg. This is likely due to the inherent variability in animal studies. Nonetheless, in aggregate, our findings largely suggest a dose-response relationship and a threshold dose for cardiac efficacy at 1×10^{14} vg/kg.

We also did not determine how long the therapeutic response to virus would be sustained. We did observe a reduction in liver VCN over time in mice injected with AAV9.LAMP2B. These findings are consistent with other AAV9 studies of the liver as well (*40*, *41*). Liver cells are more proliferative than heart or skeletal muscle cells; hence, it is expected that we see a reduction in VCN over time in this tissue. It is feasible that hepatic damage due to either viral infection or to the absence of LAMP2 may also contribute to the reduction in VCN. Hence, evaluations are ongoing to determine whether further long-term reduction in VCN occurs in the tissue types studied in the current paper.

An additional limitation regarding translation of the preclinical studies described in this paper to patients with DD is the presence of preexisting AAV9 antibodies. It is well established that these neutralizing antibodies can prevent viral transduction (*43*). In these investigations, we did not observe evidence of relevant antibodies in mice, although the prevalence of AAV antibodies may be as high as 30% in humans (*43*). Patients with such antibodies are not considered candidates for AAV9 therapies at present; however, substantial research is ongoing to address this limitation (*44*, *45*).

We did not encounter any unexpected responses/side effects after the AAV9 administration in the current study. Formal toxicology studies are ongoing. Furthermore, a phase 1 clinical trial will evaluate safety in humans. All of these studies are critical, especially given known differences in the murine and human immune response to AAV (*46*).

In summary, treatment of *Lamp2* KO mice with AAV9.LAMP2B results in robust expression of the LAMP2B transgene in the heart, liver, and skeletal muscle, the tissues most affected in DD. Furthermore, this therapy resulted in substantial improvement in tissue ultrastructure as well as metabolic and physiologic function. Additional investigations will be required to determine the long-term durability of these findings. The short-term and long-term safety and efficacy of this therapy in patients with DD are currently being evaluated in an ongoing clinical trial (ClinicalTrials.gov identifier: NCT03882437). This study includes interval histologic assessment of the cardiac and skeletal muscle after AAV9.LAMP2B administration and, hence, should address several of these critical questions.

MATERIALS AND METHODS

Study design

The goal of this study was to evaluate the efficacy of gene transfer of AAV9 carrying human *LAMP2B* cDNA (AAV9.LAMP2B) in a mouse

model of DD, the *Lamp2* KO mouse. We used 6-and 2-month-old *Lamp2* KO male mice. The 6-month-old cohort was evaluated at age 9 months (12 weeks after treatment), and the 2-month-old cohort was examined at ages 5 and 8 months (12 and 24 weeks after treatment). Untreated littermate WT mice were used as controls. The mice were randomly assigned to treatment with intravenous PBS or AAV9.LAMP2B at doses of 1×10^{13}, 5×10^{13}, 1×10^{14}, or 2×10^{14} vg/kg. All animals were subjected to intermittent fasting 6 weeks before final assessment and study termination. Cardiac contraction and relaxation were evaluated by invasive hemodynamic studies in a blind fashion. At study termination and after euthanasia, blood and tissues were collected for chemical, molecular, and histological analyses. To evaluate the efficacy of vector transduction in *Lamp2* KO compared with WT, an additional cohort of WT and *Lamp2* KO 2-month-old old male mice were injected with AAV9.LAMP2B at 2×10^{14} vg/kg and analyzed 4 weeks after injection. Sample sizes were based on previous experience with similar types of experiments in *Lamp2* KO mice (*14*). We did not exclude any animals from our experiments. Experimenters were blinded to the genotype of the specific sample to every extent possible, including during echocardiographic and hemodynamic studies as well as the toxicology studies.

AAV vector construction and production

Recombinant AAV9 vector expressing human LAMP2B was generated through a three-plasmid, helper virus–free system in collaboration with the viral vector core at the University of Pennsylvania. Transient transfection of pAAV-LAMP2B transfer plasmid, pAAV2/9 packaging plasmid, and pAd-Helper adenovirus helper plasmid into human embryonic kidney–293 producer cells generate recombinant AAV particles containing serotype 9 capsid proteins and AAV2 inverted terminal repeats (ITRs) flanking a human *LAMP2B* expression cassette (AAV9.LAMP2B). The AAV cis-transfer plasmid pAAV-LAMP2B contains the transgene expression cassette flanked by viral ITR regions derived from AAV2. The expression cassette contains the human lysosome-associated membrane glycoprotein 2 isoform B (*LAMP2B*) coding sequence driven by a chimeric promoter containing the CMV immediate-early enhancer (CMV IEE), chicken β-actin (CBA) promoter, chicken β-actin intron splice donor, and rabbit β-globin splice acceptor. The expression cassette also includes the woodchuck hepatitis posttranscriptional regulatory element (WPRE) and is terminated by the rabbit β-globin polyadenylation sequence (RGpA) (fig. S10). The fully packaged AAV particles were harvested from the culture media and concentrated by tangential flow filtration. Vector particles were subsequently purified by iodixanol gradient centrifugation, further concentrated, and buffer exchanged with final formulation buffer as previously described (*47*). Quality control assays were performed by the viral vector core at the University of Pennsylvania and include optical density (OD), $OD_{260/280}$, structure for identity, purity and DNA supercoiling identification, sequencing analysis for the plasmid (the plasmid was sequenced from ITR to ITR by Sanger's method), droplet digital PCR assay for AAV genome titer, and SDS–polyacrylamide gel electrophoresis for purity and endotoxin assay on the vectors.

Animals

All animal experiments were carried out in accordance with institutional guidelines and approved by the Institutional Animal Care and Use Committee of the University of California at San Diego. The *Lamp2* KO mice were on a C57BL/6J background.

Statistical analysis

All values are expressed as means ± SEM. GraphPad Prism 7.01 and SPSS software were used for statistical analyses. $P < 0.05$ was considered significant. Statistical significance was determined by one-way analysis of variance (ANOVA). In cases where the Brown-Forsythe test for homogeneity showed an effect of variance, Welch's one-way ANOVA was carried out, and Dunnett's post hoc test was used.

SUPPLEMENTARY MATERIALS

stm.sciencemag.org/cgi/content/full/12/535/eaax1744/DC1

Material and Methods

Fig. S1. Experimental outlines for the different experimental cohorts.

Fig. S2. Histopathology analysis on tissues from AAV9.LAMP2B-injected mice revealed no microscopic abnormalities.

Fig. S3. *Lamp2* KO mice do not have fibrosis compared with WT mice before or after AAV9.LAMP2B injection.

Fig. S4. VCN and transgene expression were not affected/changed overtime in the heart.

Fig. S5. Representative transmission electron microscopy images of cardiac tissue in the 2-month-old cohort after 24 weeks of injection.

Fig. S6. VCNs were affected/changed overtime in the liver.

Fig. S7. Administration of AAV9.LAMP2B in adolescent (2-month-old) mice shows dose-dependent expression of human LAMP2B in the liver from *Lamp2* KO mice together with an improvement in autophagic flux and in the serum measurements of ALP and ALT.

Fig. S8. Administration of AAV9.LAMP2B in 2-month-old WT and *Lamp2* KO mice shows no differences in vector transduction and transgene expression in heart and skeletal muscle between WT and *Lamp2* KO mice but decreases in the liver from *Lamp2* KO mice compared with WT.

Fig. S9. VCN and transgene expression were not affected/changed overtime in skeletal muscle.

Fig. S10. Administration of AAV9.LAMP2B in adolescent (2-month-old) mice shows dose-dependent expression of human LAMP2B in skeletal muscle from *Lamp2* KO mice together with an improvement in autophagic flux.

Fig. S11. Administration of AAV9.LAMP2B in adult (6-month-old) mice shows increased survival compared to PBS-injected controls.

Table S1. AAV9.LAMP2B vector was detected in liver, heart, and skeletal muscle.

Table S2. Antibody response against recombinant AAV9 and human LAMP2 in *Lamp2* KO mice after AAV9.LAMP2B injection.

Table S3. Morphometric analysis after AAV9.LAMP2B administration.

Table S4. Echocardiographic measurements of 6-month-old cohort male WT and *Lamp2 KO* mice after AAV9.LAMP2B treatment for 12 weeks with intermittent fasting 6 weeks before study termination.

Table S5. Administration of AAV9.LAMP2B in adult (6-month-old) and adolescent (2-month-old) *Lamp2* KO mice improved cardiac contraction and relaxation compared with PBS-injected controls.

View/request a protocol for this paper from *Bio-protocol*.

REFERENCES AND NOTES

1. C. Balmer, D. Ballhausen, N. U. Bosshard, B. Steinmann, E. Boltshauser, U. Bauersfeld, A. Superti-Furga, Familial X-linked cardiomyopathy (Danon disease): Diagnostic confirmation by mutation analysis of the *LAMP2*gene. *Eur. J. Pediatr.* **164**, 509–514 (2005).
2. J. Horvath, U.-P. Ketelsen, A. Geibel-Zehender, N. Boehm, H. Olbrich, R. Korinthenberg, H. Omran, Identification of a novel *LAMP2* mutation responsible for X-chromosomal dominant Danon disease. *Neuropediatrics* **34**, 270–273 (2003).
3. R. S. D'Souza, C. Levandowski, D. Slavov, S. L. Graw, L. A. Allen, E. Adler, L. Mestroni, M. R. G. Taylor, Danon disease: Clinical features, evaluation, and management. *Circ. Heart Fail.* **7**, 843–849 (2014).
4. P. Charron, E. Villard, P. Sébillon, P. Laforêt, T. Maisonobe, L. Duboscq-Bidot, N. Romero, V. Drouin-Garraud, T. Frébourg, P. Richard, B. Eymard, M. Komajda, Danon's disease as a cause of hypertrophic cardiomyopathy: A systematic survey. *Heart* **90**, 842–846 (2004).
5. M. Arad, B. J. Maron, J. M. Gorham, W. H. Johnson Jr., J. P. Saul, A. R. Perez-Atayde, P. Spirito, G. B. Wright, R. J. Kanter, C. E. Seidman, J. G. Seidman, Glycogen storage diseases presenting as hypertrophic cardiomyopathy. *N. Engl. J. Med.* **352**, 362–372 (2005).
6. Z. Cheng, Q. Cui, Z. Tian, H. Xie, L. Chen, L. Fang, K. Zhu, Q. Fang, Danon disease as a cause of concentric left ventricular hypertrophy in patients who underwent endomyocardial biopsy. *Eur. Heart J.* **33**, 649–656 (2012).

7. Z. Yang, C. J. McMahon, L. R. Smith, J. Bersola, A. M. Adesina, J. P. Breinholt, D. L. Kearney, W. J. Dreyer, S. W. Denfield, J. F. Price, M. Grenier, N. J. Kertesz, S. K. Clunie, S. D. Fernbach, J. F. Southern, S. Berger, J. A. Towbin, K. R. Bowles, N. E. Bowles, Danon disease as an underrecognized cause of hypertrophic cardiomyopathy in children. *Circulation* **112**, 1612–1617 (2005).
8. A. A. Alfares, M. A. Kelly, G. McDermott, B. H. Funke, M. S. Lebo, S. B. Baxter, J. Shen, H. M. McLaughlin, E. H. Clark, L. J. Babb, S. W. Cox, S. R. DePalma, C. Y. Ho, J. G. Seidman, C. E. Seidman, H. L. Rehm, Results of clinical genetic testing of 2,912 probands with hypertrophic cardiomyopathy: Expanded panels offer limited additional sensitivity. *Genet. Med.* **17**, 880–888 (2015).
9. E.-L. Eskelinen, Roles of LAMP-1 and LAMP-2 in lysosome biogenesis and autophagy. *Mol. Aspects Med.* **27**, 495–502 (2006).
10. E.-L. Eskelinen, A. L. Illert, Y. Tanaka, G. Schwarzmann, J. Blanz, K. von Figura, P. Saftig, Role of LAMP-2 in lysosome biogenesis and autophagy. *Mol. Biol. Cell* **13**, 3355–3368 (2002).
11. C. Chi, A. Leonard, W. E. Knight, K. M. Beussman, Y. Zhao, Y. Cao, P. Londono, E. Aune, M. A. Trembley, E. M. Small, M. Y. Jeong, L. A. Walker, H. Xu, N. J. Sniadecki, M. R. Taylor, P. M. Buttrick, K. Song, LAMP-2B regulates human cardiomyocyte function by mediating autophagosome–lysosome fusion. *Proc. Natl. Acad. Sci. U.S.A.* **116**, 556–565 (2019).
12. D. Hong, Z. Shi, W. Zhang, Z. Wang, Y. Yuan, in *Clinical Neuropathology* (Dustri-Verlag, 2012).
13. S. I. Hashem, C. N. Perry, M. Bauer, S. Han, S. D. Clegg, K. Ouyang, D. C. Deacon, M. Spinharney, A. D. Panopoulos, J. C. I. Belmonte, K. A. Frazer, J. Chen, Q. Gong, Z. Zhou, N. C. Chi, E. D. Adler, Oxidative stress mediates cardiomyocyte apoptosis in a human model of Danon disease and heart failure. *Stem Cells* **33**, 2343–2350 (2015).
14. S. I. Hashem, A. N. Murphy, A. S. Divakaruni, M. L. Klos, B. C. Nelson, E. C. Gault, T. J. Rowland, C. N. Perry, Y. Gu, N. D. Dalton, W. H. Bradford, E. J. Devaney, K. L. Peterson, K. L. Jones, M. R. G. Taylor, J. Chen, N. C. Chi, E. D. Adler, Impaired mitophagy facilitates mitochondrial damage in Danon disease. *J. Mol. Cell. Cardiol.* **108**, 86–94 (2017).
15. S. Zacchigna, L. Zentilin, M. Giacca, Adeno-associated virus vectors as therapeutic and investigational tools in the cardiovascular system. *Circ. Res.* **114**, 1827–1846 (2014).
16. C. Mah, C. A. Pacak, K. O. Cresawn, L. R. DeRuisseau, S. Germain, M. A. Lewis, D. A. Cloutier, D. D. Fuller, B. J. Byrne, Physiological correction of Pompe disease by systemic delivery of adeno-associated virus serotype 1 vectors. *Mol. Ther.* **15**, 501–507 (2007).
17. C. Zincarelli, S. Soltys, G. Rengo, J. E. Rabinowitz, Analysis of AAV serotypes 1-9 mediated gene expression and tropism in mice after systemic injection. *Mol. Ther.* **16**, 1073–1080 (2008).
18. M. E. Hester, K. D. Foust, R. W. Kaspar, B. K. Kaspar, AAV as a gene transfer vector for the treatment of neurological disorders: Novel treatment thoughts for ALS. *Curr. Gene Ther.* **9**, 428–433 (2009).
19. J. Lovric, M. Mano, L. Zentilin, A. Eulalio, S. Zacchigna, M. Giacca, Terminal differentiation of cardiac and skeletal myocytes induces permissivity to AAV transduction by relieving inhibition imposed by DNA damage response proteins. *Mol. Ther.* **20**, 2087–2097 (2012).
20. A. S. Meadows, F. J. Duncan, M. Camboni, K. Waligura, C. Montgomery, K. Zaraspe, B. J. Naughton, W. G. Bremer, C. Shilling, C. M. Walker, B. Bolon, K. M. Flanigan, K. L. Mc Bride, D. M. McCarty, H. Fu, A GLP-compliant toxicology and biodistribution study: Systemic delivery of a rAAV9 vector for the treatment of mucopolysaccharidosis IIIB. *Hum. Gene Ther. Clin. Dev.* **2015**, 228–242 (2015).
21. Y. Tanaka, G. Guhde, A. Suter, E.-L. Eskelinen, D. Hartmann, R. Lüllmann-Rauch, P. M. L. Janssen, J. Blanz, K. von Figura, P. Saftig, Accumulation of autophagic vacuoles and cardiomyopathy in LAMP-2-deficient mice. *Nature* **406**, 902–906 (2000).
22. T. J. Rowland, M. E. Sweet, L. Mestroni, M. R. G. Taylor, Danon disease – dysregulation of autophagy in a multisystem disorder with cardiomyopathy. *J. Cell Sci.* **129**, 2135–2143 (2016).
23. K. Sugie, A. Yamamoto, K. Murayama, S. J. Oh, M. Takahashi, M. Mora, J. E. Riggs, J. Colomer, C. Iturriaga, A. Meloni, C. Lamperti, S. Saitoh, E. Byrne, S. DiMauro, I. Nonaka, M. Hirano, I. Nishino, Clinicopathological features of genetically confirmed Danon disease. *Neurology* **58**, 1773–1778 (2002).
24. M. Brambatti, O. Caspi, A. Maolo, E. Koshi, B. Greenberg, M. R. G. Taylor, E. D. Adler, Danon disease: Gender differences in presentation and outcomes. *Int. J. Cardiol.* **286**, 92–98 (2019).
25. J. Stypmann, P. M. L. Janssen, J. Prestle, M. A. Engelen, H. Kögler, R. Lüllmann-Rauch, L. Eckardt, K. von Figura, J. Landgrebe, A. Mleczko, P. Saftig, LAMP-2 deficient mice show depressed cardiac contractile function without significant changes in calcium handling. *Basic Res. Cardiol.* **101**, 281–291 (2006).
26. R. J. Godar, X. Ma, H. Liu, J. T. Murphy, C. J. Weinheimer, A. Kovacs, S. D. Crosby, P. Saftig, A. Diwan, Repetitive stimulation of autophagy-lysosome machinery by intermittent fasting preconditions the myocardium to ischemia-reperfusion injury. *Autophagy* **11**, 1537–1560 (2015).
27. S. Sciarretta, N. Hariharan, Y. Monden, D. Zablocki, J. Sadoshima, Is autophagy in response to ischemia and reperfusion protective or detrimental for the heart? *Pediatr. Cardiol.* **32**, 275–281 (2011).
28. D. A. Murrey, B. J. Naughton, F. J. Duncan, A. S. Meadows, T. A. Ware, K. J. Campbell, W. G. Bremer, C. M. Walker, L. Goodchild, B. Bolon, K. La Perle, K. M. Flanigan, K. L. McBride, D. M. McCarty, H. Fu, Feasibility and safety of systemic rAAV9-h*NAGLU* delivery for treating mucopolysaccharidosis IIIB: Toxicology, biodistribution, and immunological assessments in primates. *Hum. Gene. Ther. Clin. Dev.* **25**, 72–84 (2014).
29. C. B. McLeland, J. Rodriguez, S. T. Stern, Autophagy monitoring assay: Qualitative analysis of MAP LC3-I to II conversion by immunoblot. *Methods Mol. Biol.* **697**, 199–206 (2011).
30. L. Wang, J. Wang, W. Cai, Y. Shi, X. Zhou, G. Guo, C. Guo, X. Huang, Z. Han, S. Zhang, S. Ma, X. Zhou, D. Fan, M. E. Gershwin, Y. Han, A critical evaluation of liver pathology in humans with Danon disease and experimental correlates in a rat model of LAMP-2 deficiency. *Clin. Rev. Allergy Immunol.* **53**, 105–116 (2017).
31. S. Ma, M. Zhang, S. Zhang, J. Wang, X. Zhou, G. Guo, L. Wang, M. Wang, Z. Peng, C. Guo, X. Zheng, X. Zhou, J. Wang, Y. Han, Characterisation of Lamp2-deficient rats for potential new animal model of Danon disease. *Sci. Rep.* **8**, 6932 (2018).
32. S. C. Cunningham, A. P. Dane, A. Spinoulas, I. E. Alexander, Gene delivery to the juvenile mouse liver using AAV2/8 vectors. *Mol. Ther.* **16**, 1081–1088 (2008).
33. M. C. V. Malicdan, I. Nishino, Autophagy in lysosomal myopathies. *Brain Pathol.* **22**, 82–88 (2012).
34. Y. Endo, A. Furuta, I. Nishino, Danon disease: A phenotypic expression of LAMP-2 deficiency. *Acta Neuropathol.* **129**, 391–398 (2015).
35. A. C. Nascimbeni, M. Fanin, C. Angelini, M. Sandri, Autophagy dysregulation in Danon disease. *Cell Death Dis.* **8**, e2565 (2018).
36. M. Rothaug, S. Stroobants, M. Schweizer, J. Peters, F. Zunke, M. Allerding, R. D'Hooge, P. Saftig, J. Blanz, LAMP-2 deficiency leads to hippocampal dysfunction but normal clearance of neuronal substrates of chaperone-mediated autophagy in a mouse model for Danon disease. *Acta Neuropathol. Commun.* **3**, 6 (2015).
37. C. Hinderer, N. Katz, E. L. Buza, C. Dyer, T. Goode, P. Bell, L. K. Richman, J. M. Wilson, Severe toxicity in nonhuman primates and piglets following high-dose intravenous administration of an adeno-associated virus vector expressing human SMN. *Hum. Gene Ther.* **29**, 285–298 (2018).
38. A. S. Meadows, F. J. Duncan, M. Camboni, K. Waligura, C. Montgomery, K. Zaraspe, B. J. Naughton, W. G. Bremer, C. Shilling, C. M. Walker, B. Bolon, K. M. Flanigan, K. L. McBride, D. M. McCarty, H. Fu, A GLP-compliant toxicology and biodistribution study: Systemic delivery of an rAAV9 vector for the treatment of mucopolysaccharidosis IIIB. *Hum. Gene. Ther. Clin. Dev.* **26**, 228–242 (2015).
39. J. L. Schneider, Y. Suh, A. M. Cuervo, Deficient chaperone-mediated autophagy in liver leads to metabolic dysregulation. *Cell Metab.* **20**, 417–432 (2014).
40. G. Bortolussi, L. Zentillin, J. Vaníkova, L. Bockor, C. Bellarosa, A. Mancarella, E. Vianello, C. Tiribelli, M. Giacca, L. Vitek, A. F. Muro, Life-long correction of hyperbilirubinemia with a neonatal liver-specific AAV-mediated gene transfer in a lethal mouse model of Crigler–Najjar syndrome. *Hum. Gene Ther.* **25**, 844–855 (2014).
41. L. Wang, H. Wang, P. Bell, D. McMenamin, J. M. Wilson, Hepatic gene transfer in neonatal mice by adeno-associated virus serotype 8 vector. *Hum. Gene Ther.* **23**, 533–539 (2012).
42. S. Kaushik, A. M. Cuervo, The coming of age of chaperone-mediated autophagy. *Nat. Rev. Mol. Cell Biol.* **19**, 365–381 (2018).
43. K. Rapti, V. Louis-Jeune, E. Kohlbrenner, K. Ishikawa, D. Ladage, S. Zolotukhin, R. J. Hajjar, T. Weber, Neutralizing antibodies against AAV serotypes 1, 2, 6, and 9 in sera of commonly used animal models. *Mol. Ther.* **20**, 73–83 (2012).
44. D. Katrekar, A. M. Moreno, G. Chen, A. Worlikar, P. Mali, Oligonucleotide conjugated multi-functional adeno-associated viruses. *Sci. Rep.* **8**, 3589 (2018).
45. R. E. Kelemen, S. B. Erickson, A. Chatterjee, Production and chemoselective modification of adeno-associated virus site-specifically incorporating an unnatural amino acid residue into its capsid. *Methods Mol. Biol.* **1728**, 313–326 (2018).
46. J. Rabinowitz, Y. K. Chan, R. J. Samulski, Adeno-associated virus (AAV) versus immune response. *Viruses* **11**, 102 (2019).
47. M. Lock, M. Alvira, L. H. Vandenberghe, A. Samanta, J. Toelen, Z. Debyser, J. M. Wilson, Rapid, simple, and versatile manufacturing of recombinant adeno-associated viral vectors at scale. *Hum. Gene Ther.* **21**, 1259–1271 (2010).

Acknowledgments: We thank all the members of Adler's laboratory and members of the UCSD Molecular Biology Program for constructive criticism. We also thank the UPenn vector core for the AAV9 production, the Illinois Institute of Technology Research Institute for ADA assays and histopathology from different organs, and the Texas Heart Institute for electron microscopy images on the supplementary figures. **Funding:** This work was supported by an unrestricted grant from the H. S. Lopez Family Foundation founded by C. S. Lopez and H. S. Lopez and a Sponsored Research agreement from Rocket Pharmaceuticals Inc. S.I.H. was supported by American Heart Association postdoctoral fellowship 16POST29740010. The electron micrographs were taken in the Cellular and Molecular Medicine Electron microscopy core facility, which is supported in part by NIH award number S10OD023527. Confocal microscopy was performed at the UCSD School of Medicine Microscopy Core, which is supported by a NINDS P30 grant (NS047101). **Author contributions:** A.M.M. carried

out the experiments and wrote and revised the manuscript. S.I.H. carried out the preliminary experiments and assisted with the experimental design. B.C.N. assisted with the design of the viral vector and assisted with the experimental design and manuscript revision. E.G. and A.S.-H. performed murine experiments and assisted with interpretation. M.B. and J.B. assisted with statistical analysis. E.V. and C.C. provided technical help and assistance. P.J.B. assisted with manuscript revision. P.B., A.K., J.D.S., and G.S. assisted with the experimental design and manuscript revision. Y.G. performed cardiac catheterization and data analysis. N.D.D. performed transthoracic echocardiography and data analysis. K.H assisted with vector design, experimental design, and interpretation. K.P. assisted with the design and interpretation of results. P.S. provided *Lamp2* KO mice and assisted with manuscript revision. E.D.A. conceived the project, supervised all experiments, and wrote and revised the manuscript. **Competing interests:** E.D.A., S.I.H, and B.C.N. are inventors on a patent entitle "Methods for the treatment of Danon disease and other disorders of autophagy" (#2017127565A1). E.D.A. is a shareholder of Rocket Pharmaceuticals. He is a consultant for Fujifilm, Ionis, Medtronic, Novartis, Abbott Healthcare, and Abiomed and a cofounder and shareholder of GenStem Therapeutics. A.M.M. and M.B. are consultants for Rocket Pharmaceuticals. P.B., A.K., J.D.S., and G.S. are employees of Rocket Pharmaceuticals. **Data and materials availability:** Reagents and mouse models described here are accessible through a material transfer agreement. All data associated with this study are present in the paper or the Supplementary Materials.

Submitted 28 February 2019
Resubmitted 18 August 2019
Accepted 20 February 2020
Published 18 March 2020
10.1126/scitranslmed.aax1744

Citation: A. M. Manso, S. I. Hashem, B. C. Nelson, E. Gault, A. Soto-Hermida, E. Villarruel, M. Brambatti, J. Bogomolovas, P. J. Bushway, C. Chen, P. Battiprolu, A. Keravala, J. D. Schwartz, G. Shah, Y. Gu, N. D. Dalton, K. Hammond, K. Peterson, P. Saftig, E. D. Adler, Systemic AAV9.LAMP2B injection reverses metabolic and physiologic multiorgan dysfunction in a murine model of Danon disease. *Sci. Transl. Med.* **12**, eaax1744 (2020).

Science Translational Medicine

Systemic AAV9.LAMP2B injection reverses metabolic and physiologic multiorgan dysfunction in a murine model of Danon disease

Ana Maria Manso, Sherin I. Hashem, Bradley C. Nelson, Emily Gault, Angel Soto-Hermida, Elizza Villarruel, Michela Brambatti, Julius Bogomolovas, Paul J. Bushway, Chao Chen, Pavan Battiprolu, Annahita Keravala, Jonathan D. Schwartz, Gaurav Shah, Yusu Gu, Nancy D. Dalton, Kirk Hammond, Kirk Peterson, Paul Saftig and Eric D. Adler

Sci Transl Med **12**, eaax1744.
DOI: 10.1126/scitranslmed.aax1744

Switching on the *LAMP*(*2B*)

Mutations in the in the lysosomal-associated membrane protein 2 (LAMP2) cause Danon disease (DD), a rare X-linked myopathy associated with weakening of skeletal and heart muscles, multiorgan dysfunction, and intellectual disability. Currently, there is no specific treatment. Now, Manso *et al.* tested the efficacy of adeno-associated virus 9 (AAV9)–mediated gene therapy delivering the human *LAMP2B* gene in *Lamp2* KO mice, a model of DD. AAV9.LAMP2B injected systemically in mice restored protein expression in multiple organs, improved metabolic abnormalities and cardiac function, and increased survival. The results suggest that gene therapy delivery *LAMP2B* might be a therapeutic option for patients with DD.